Wind speed climatology and trends for Australia, 1975–2006: Capturing the stilling phenomenon and comparison with near-surface reanalysis output

Tim R. McVicar,[1] Thomas G. Van Niel,[2] Ling Tao Li,[1] Michael L. Roderick,[3] David P. Rayner,[4] Lucrezia Ricciardulli,[5] and Randall J. Donohue[1]

Received 10 August 2008; revised 9 September 2008; accepted 18 September 2008; published 18 October 2008.

[1] Near-surface wind speeds (u) measured by terrestrial anemometers show declines (a 'stilling') at a range of mid-latitude sites, but two gridded u datasets (a NCEP/NCAR reanalysis output and a surface-pressure-based u model) have not reproduced the stilling observed at Australian stations. We developed Australia-wide 0.01° resolution daily u grids by interpolating measurements from an expanded anemometer network for 1975–2006. These new grids represented the magnitude and spatial-variability of observed u trends, whereas grids from reanalysis systems (NCEP/NCAR, NCEP/DOE and ERA40) essentially did not, even when minimising the sea-breeze impact. For these new grids, the Australian-averaged u trend for 1975–2006 was -0.009 m s^{-1} a^{-1} (agreeing with earlier site-based studies) with stilling over 88% of the land-surface. This new dataset can be used in numerous environmental applications, including benchmarking general circulation models to improve the representation of key parameters that govern u estimation. The methodology implemented here can be applied globally. **Citation:** McVicar, T. R., T. G. Van Niel, L. T. Li, M. L. Roderick, D. P. Rayner, L. Ricciardulli, and R. J. Donohue (2008), Wind speed climatology and trends for Australia, 1975–2006: Capturing the stilling phenomenon and comparison with near-surface reanalysis output, *Geophys. Res. Lett.*, *35*, L20403, doi:10.1029/2008GL035627.

1. Introduction

[2] Recent observations of near-surface wind speed (u) trends measured by terrestrial anemometers have shown declines between -0.004 m s^{-1} a^{-1} to -0.017 m s^{-1} a^{-1} (with an average of approximately -0.010 m s^{-1} a^{-1}) over the last 30 to 50 years for a range of mid-latitude regions including: Australia [*Roderick et al.*, 2007]; China [*Xu et al.*, 2006a, 2006b]; Europe [*Pirazzoli and Tomasin*, 2003]; North America [*Hobbins*, 2004; *Klink*, 1999; *Tuller*, 2004]; and Tibet [*Shenbin et al.*, 2006; *Zhang et al.*, 2007]. Others report different u metrics also showing decreases: (i) *Pryor et al.* [2007] report that over the contiguous USA the annual median u decreased significantly (P = 0.1) for 118 (out of 157) stations for 1973–2005; and (ii) *Smits et al.* [2005] show that the frequency of weak and moderate storm events at 13 Dutch stations for 1962–2002 decreased by approximately 20% and 10% per decade, respectively. In contrast, high-latitude (> 65°) sites in Antarctica [*Aristidi et al.*, 2005; *Turner et al.*, 2005] and Alaska [*Lynch et al.*, 2004] report increases of approximately 0.005 m s^{-1} a^{-1}. This latitudinal dependence of u trends agrees with model projections showing decreasing u at mid-latitudes with increasing u at high-latitudes [*Seidel et al.*, 2008; *Yin*, 2005].

[3] In Australia, two studies recently illustrated that declining u from 1975–2004 is the primary factor reducing atmospheric evaporative demand, as measured by pan evaporation [*Rayner*, 2007; *Roderick et al.*, 2007]; with the term 'stilling' being coined to denote the negative u trend [*Roderick et al.*, 2007]. *Rayner* [2007] found that two gridded u datasets (NCEP/NCAR reanalysis output and a surface-pressure-based model) did not capture the observed stilling. Thus it remains possible that the site-based data used in the above-mentioned Australian pan evaporation studies are not representative of regional conditions because the non-uniform spatial distribution of the long record u observations makes their aggregation into an 'Australia-wide' trend questionable. More generally, the results from all other studies are only based on averaging across sites with no regard for the spatial representation of the sites. To address this limitation requires the generation of a time-series of surfaces, and as the u trends are of sufficient magnitude to be important for climate change, wind power generation and water resource assessments, more detailed investigation is warranted. Here we report the development of high-resolution (0.01°) daily u grids using an expanded anemometer database for the entire Australian land-surface covering 7.6 million km^2 (10–45°S and 110–155°E). Annual u trends were calculated from these new surfaces and compared against trends from earlier studies and with outputs from three commonly used reanalysis systems (NCEP/NCAR, NCEP/DOE and ERA40).

2. Materials and Methods

[4] Daily wind run data (km day^{-1}) for low-set anemometers (2 m) were acquired from the Australian *Bureau of Meteorology* [2007] from 1 Jan 1975 through 31 Dec 2006 (32 years totalling 11,688 days). The data and associated quality control flags were shuffled backward one day, as observations were made at 0900 local time each day with the

[1]CSIRO Land and Water and eWater Cooperative Research Centre, Canberra, A.C.T., Australia.
[2]CSIRO Land and Water and eWater Cooperative Research Centre, Wembley, Western Australia, Australia.
[3]Research School of Earth Sciences, Australian National University, Canberra, A.C.T., Australia.
[4]Department of Earth Sciences, University of Gothenburg, Gothenburg, Sweden.
[5]Remote Sensing Systems, Santa Rosa, California, USA.

0094-8276/08/2008GL035627$05.00

majority of the wind-run generally occurring in the afternoon of the previous day [*Archer and Jacobson*, 2003; *Rehman and Ahmad*, 2004]. Daily wind run data were excluded if: (i) quality control flags indicated that they were considered wrong, suspect, or inconsistent with other known information; (ii) data were accumulated over two or more days; or (iii) wind run exceeded 1200 km day^{-1} [*Rayner*, 2007]. The data were converted from km day^{-1} to daily average u with units of m s^{-1}. The number of sites available on any given day varied from 112 to 194, having an overall average of 163 stations. Most sites were located within 45 km of the coast (input data are characterised in Figures S1 and S2 and Table S1).[1]

[5] Daily data were spatially interpolated using ANUSPLIN (version 4.3) [*Hutchinson*, 2004]. The wide-spread use of ANUSPLIN for interpolating hydrometeorological and climatological data, and its advantages over other approaches, are summarised by *McVicar et al.* [2007]. To fit the daily u data, four models were tested with the trivariate thin-plate spline as a function of longitude, latitude and distance inland from coast [*Hutchinson et al.*, 1984] providing the best statistical fits (see Text S1, Figure S3, and Tables S2, S3, and S4 for details). The 11,688 daily u surfaces were output with a 0.01° (approximately 1 km) resolution to accurately represent sea-breezes and to match similar resolution remotely sensed data that are used in actual and potential evapotranspiration modelling.

[6] Monthly average u surfaces were derived from the daily surfaces for each of the 384 months, and from these, monthly, seasonal and annual climatologies were generated for the 32 years. Trend analysis was performed on monthly, seasonal and annual time series by fitting a linear regression (ordinary least squares) to each grid-cell with significance ($P = 0.05$) being determined using a two-tailed t-test.

[7] Annual climatologies and trend statistics were developed for: (1) the new surfaces generated herein; and 10 m high reanalysis winds from (2) the National Centers for Environmental Prediction Department of Energy (NCEP/DOE [*Kanamitsu et al.*, 2002]; http://www.cdc.noaa.gov/cdc/data.ncep.reanalysis2.html); (3) NCEP National Center for Atmospheric Research (NCEP/NCAR [*Kalnay et al.*, 1996]; http://www.cdc.noaa.gov/cdc/data.ncep.reanalysis.html); and (4) European Centre for Medium-range Weather Forecasts (ECMWF) 40 Years Re-Analysis (ERA40 [*Uppala et al.*, 2005]; http://data.ecmwf.int/data/d/era40_daily). For (2) to (4), we downloaded sub-daily, non-averaged wind vectors and created sub-daily u. These were then averaged to monthly u and resampled to a common 2° resolution, then annual u climatologies and trends were derived. The reanalysis products were all 10 m height, whereas the anemometer observations were at 2 m. Assuming: (i) a logarithmic u profile [*Robeson and Shein*, 1997; *Stull*, 1988]; (ii) that the profile is constant through time; (iii) neutral atmospheric stability; and (iv) a typical range of roughness values (i.e., varying from 0.1 m [*Stull*, 1988] to 0.65 m [*Stull*, 1994]), it is expected that 10 m u and u trends will be between 1.5 to 2.4 times larger than those at 2 m. To minimise sea/land-breeze effects [*Stull*, 1988], we also calculated climatologies and trends using 'land-only' grid-cells, with our data resampled to the common 2° resolution. Finally, the u trends observed at 41 BoM stations [*Roderick et al.*, 2007] across Australia were compared against data extracted from (1) to (4) above. All the above comparisons were made for the period 1979–2001 (the ERA40 data extent). *Rayner* [2007] used NCEP/NCAR 0.995-sigma surfaces, transferred to 2 m height using a static wind power profile relationship to assess u trends at points. Our research extends this by: (i) assessing output from all three reanalysis systems; (ii) implementing a vertical transfer based only on height (not a mixed height-pressure transfer that does not account for surface pressure changes); and (iii) performing analyses using both grids and points.

3. Results

[8] Annual climatology (Figure 1a) shows higher u associated with arid regions and lower u associated with wetter coastal regions. The Australian-average u (Figure 1b) ranged between 2.3 m s^{-1} in summer (DJF) to 1.7 m s^{-1} in winter (JJA); see Table S5 and Figure S4. While all-Australian monthly averages are fairly constant (Figure 1b), some local differences associated with processes governing Australia's climate (e.g., the summer-winter latitudinal movement of the sub-tropical ridge) are clearly seen (Figure 1c).

[9] Figure 1d shows the distribution of annual u trends for 1975–2006. The majority (88.6%) of Australia exhibits stilling, with 57.5% of grid-cells having negative and significant ($P = 0.05$) trends; the majority of annual, seasonal and monthly significant trends are negative (Table S6). The average annual trend of −0.009 m s^{-1} a^{-1} is very similar to the −0.010 m s^{-1} a^{-1} calculated by *Roderick et al.* [2007] by averaging the results across 41 BoM stations for 1975–2004. Monthly average (Figure 1e), point (Figure 1f), and extreme monthly grid-cell (Table S6) u trends are similar to those reported for other mid-latitude sites. The seasonal (Figure S5) and annual (Figure 1d) u trends have similar spatial patterns except for increasing u trends in autumn and winter found in north-eastern Queensland, which are associated with a positive phase of the Southern Annular Mode [*Gillett et al.*, 2006; *Hendon et al.*, 2007].

[10] The reanalysis-based u climatologies are 1.85 to 2.25 times larger than our data (Table 1), as expected given the height differences (see above). Table 1 also shows that the Australian-averaged reanalysis-based u trends are three to six times smaller than for our data. The results are similar when comparing land-only grid cells of equal 2° resolution (Table S7), so this reanalysis-based u trend underestimation cannot be explained as a sea/land-breeze effect.

[11] Figure 2 shows that the u trends determined using our interpolation and analysis process captured the trend better than the three reanalysis products ($r^2 = 0.380$ compared with r^2 from 0.001 to 0.008). Table 1 also shows that the observed u trends are poorly captured in the reanalysis output. This suggests: (i) changes in the reanalysis data assimilation have acted to mask the observed u changes; and/or (ii) an inadequate representation of key boundary-layer parameters in the reanalysis systems that govern u estimation.

4. Discussion

[12] After spatial interpolation using an expanded database, we found similar stilling as reported previously using

[1] Auxiliary materials are available in the HTML. doi:10.1029/2008GL035627.

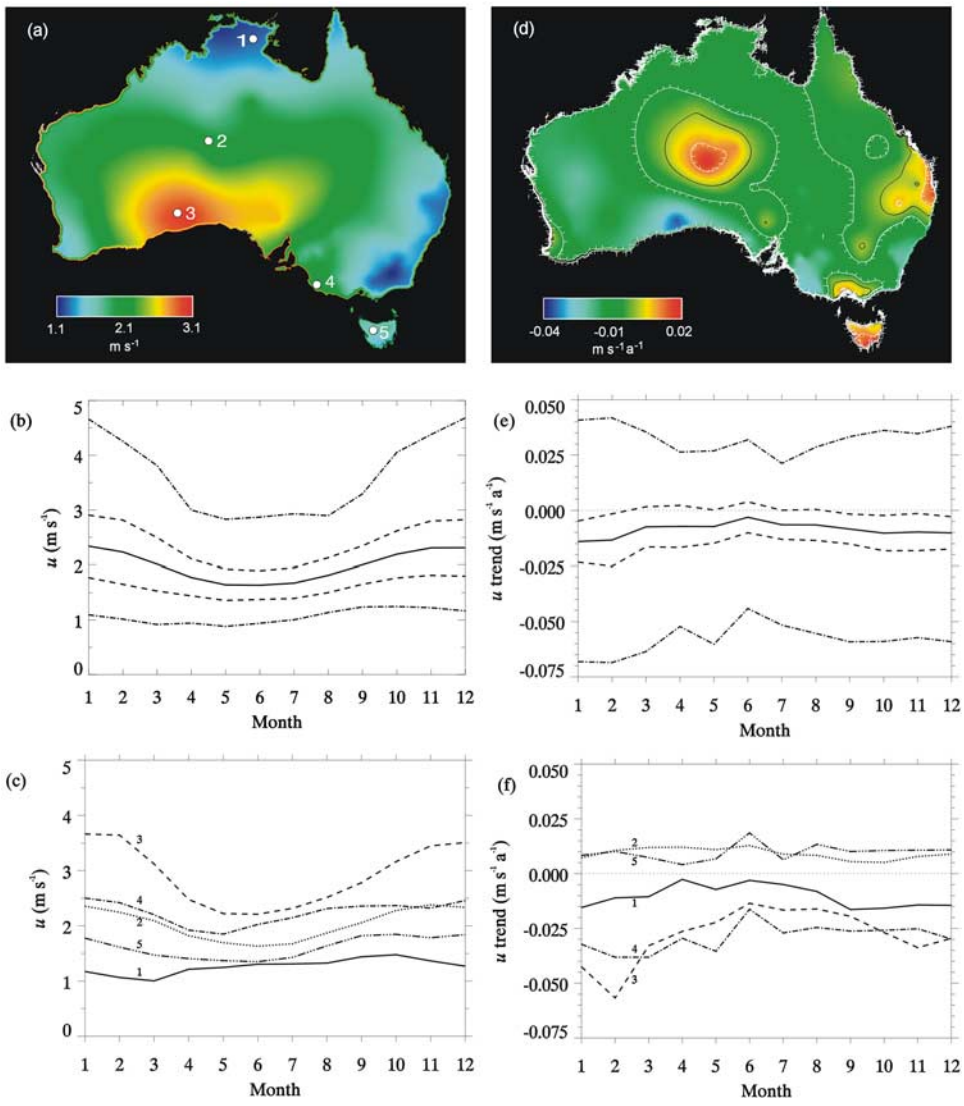

Figure 1. Climatology and trends for u 1975–2006: (a) annual climatology; (b) continent-averaged monthly climatology; (c) monthly climatology for the five points shown in Figure 1a; (d) annual trend; (e) continent-averaged monthly trends; and (f) monthly trends for the five points shown in Figure 1a. In Figure 1a the locations are: (1) 134.5°E, 13.5°S; (2) 130.0°E, 22.5°S; (3) 127.0°E, 30.5°S; (4) 140.5°E, 37.5°S; and (5) 146.0°E, 42.0°S. In Figure 1b and 1e the 32-year mean (solid line), ±1 standard deviation (dashed lines), and the minimum and maximum (dash–dot lines) are shown. In Figure 1d the black line shows where the trend is 0.0 m s^{-1} a^{-1} and the white lines show where the trends change from being non-significant to significant (P = 0.05); the white barbs are in the direction of significance.

individual station data from 41 BoM sites across Australia [*Roderick et al.*, 2007]. Over the 1975–2006 period, the majority of Australia (~ 88% of the continental surface) experienced stilling (Table S6). Over the remaining 12% of the continent, our results show increasing u in three distinct regions (Figure 1d): (i) central Australia; (ii) southeast Queensland and northeast New South Wales; and (iii) southern Victoria and Tasmania. In arid central Australia, there was exceptionally high precipitation during the mid-1970s coincident with the start of the period analysed here. During the mid-1970s, more of the available energy would have been partitioned into the latent heat flux (and associated with increased vegetation growth) than the sensible heat flux (and associated turbulent transport) [*Roderick et al.*, 2007, Figure S3c] resulting in lower u [*Ozdogan et al.*,

Table 1. Australian-Average Annual u Climatology and Trends for 1979–2001[a]

Source	Mean	Std Dev	Max.	Min.	Num Grid-Cells	Mean Relative to Our Mean
			Climatology			
Our study	1.99	0.40	3.44	1.14	6,979,336	1.00
NCEP/DOE	4.48	0.96	8.68	2.52	185	2.25
NCEP/NCAR	3.67	0.99	8.68	1.91	185	1.84
ERA40	3.80	0.67	7.21	2.38	185	1.91
			Trends			
Our study	−0.013	0.010	0.047	−0.059	6,979,336	1.00
NCEP/DOE	−0.002	0.007	0.012	−0.038	185	0.15
NCEP/NCAR	−0.004	0.004	0.007	−0.019	185	0.31
ERA40	−0.002	0.007	0.034	−0.020	185	0.15

[a]The units of the climatology data are m s^{-1} and the units of the trend data are m s^{-1} a^{-1}.

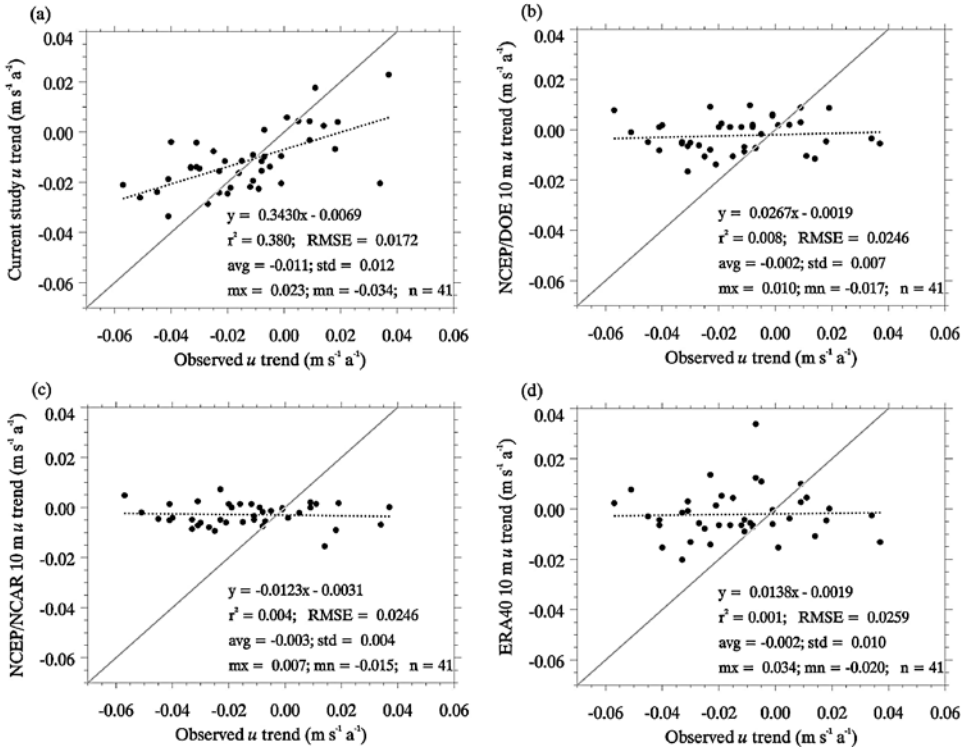

Figure 2. Comparison of wind speed trends at the 41 BoM sites used by *Roderick et al.* [2007] for 1979–2001 with trends extracted from: (a) this study; (b) NCEP/DOE 10 m output; (c) NCEP/NCAR 10 m output; and (d) ERA40 10 m output. At the 41 BoM sites, statistics for 1979–2001 are average (avg) = −0.013, standard deviation (std) = 0.022, maximum (mx) = 0.037, and minimum (mn) = −0.057; all units are m s^{-1} a^{-1}. For each plot, the line of best fit is the dotted black line defined by the equation, the 1:1 line is gray, and the avg, std, mx and mn (all units are m s^{-1} a^{-1}) of the Y-axis data are shown. The units of all offsets and RMSE statistics are m s^{-1} a^{-1}, whereas r^2 and slope statistics are unitless.

2006] at the start of the period. If the analysis period had begun in 1980, instead of 1975, the increase in central Australia would not be present. The two other regions identified in Figure 1d warrant further investigation: increasing *u* trends in southeast Queensland and northeast New South Wales could be associated with decreased precipitation and/or rapid urbanisation changing local circulation patterns, and trends in southern Victoria and Tasmania are likely influenced by the Southern Annular Mode [*Gupta and England*, 2006; *Hendon et al.*, 2007].

[13] The finding that annually over 88% of Australia showed stilling, with 57% (Table S6) being statistically significant (P = 0.05), demonstrates a high degree of spatial coherence in the input *u* observations, which suggests that regional (or global) processes dominate the 'potential local factors' (e.g., growing trees or other obstacles progressively obstructing the air flow) discussed by *Roderick et al.* [2007]. This raises a very interesting question because there is a wealth of evidence from terrestrial anemometer records showing that regionally-averaged declines in *u* are prevalent at mid-latitudes with increases typical at high-latitudes (see Introduction). This basic pattern of change is also shown by climate change projections [*Lorenz and DeWeaver*, 2007; *Yin*, 2005] and has been associated with poleward expansions of the Hadley cell [*Lu et al.*, 2007; *Seidel et al.*, 2008].

[14] In contrast, *Wentz et al.* [2007] reported that *u* averaged over the global oceans increased by 0.008 m s^{-1} a^{-1} for 1987–2006, based on passive microwave satellite retrievals. Closer to the equator (oceans between 30°S and 30°N), they report a lower but still increasing trend of 0.004 m s^{-1} a^{-1}. Hence those data also suggest latitudinally-dependent *u* changes, although there is still no reconciliation on how *u* could increase over the ocean while decreasing over the land in the mid-latitudes.

[15] The importance of *u* trends for predicting the interacting feedbacks between trends of precipitation, temperature and vapor pressure has recently been highlighted by the climate change community [*Allan and Soden*, 2007; *Held and Soden*, 2006; *Wentz et al.*, 2007]. Therefore further measurement and modelling in other regions are needed to place terrestrial stilling in a wider context: focussing on spatial (e.g., tropical latitudes for terrestrial- and oceanic-surfaces); vertical (e.g., to at least 80 m, the typical height of commercial wind turbines [*Archer and Jacobson*, 2003; *Pérez et al.*, 2005]); and temporal aspects.

[16] It is concerning that the terrestrial stilling is so poorly represented by the reanalysis outputs, as the representation of the key boundary layer parameters that govern *u* estimates in the reanalysis models is likely similar to the circulation models used to predict climate change. A recent validation study of ERA40 and NCEP/DOE near-surface outputs did not consider *u* [*Betts et al.*, 2006] whereas our validation results of *u* for Australia suggests further measurement and modelling need to be extended to a wider

context (see above) as a matter of high priority. The methodology used here can be implemented to the global land-surface and so can play an important role in providing verification data for such a study.

5. Conclusion

[17] Using anemometer observations from approximately 160 sites, daily surfaces of u have been interpolated for the Australian continent for 1975–2006. The results showed reductions in u over some 88% of the continent. Averaged over the continent, the trend was -0.009 m s^{-1} a^{-1}, in general agreement with earlier site-based studies. Taking into account height differences, the u climatology of the gridded surfaces was generally consistent with the NCEP/NCAR, NCEP/DOE and ERA40 reanalysis products, but the observed u trends were essentially not captured in any of these. Densities of anemometers similar to that of Australia are likely found for many other parts of the global land-surface, so our methodology provides an avenue to develop daily u grids elsewhere. By capturing the stilling trends in Australia, the resultant surfaces provide a benchmark retrospective dataset that general circulation model output can be compared with. Additionally, the surfaces can be used in numerous applications including the estimation of evapotranspiration [*McVicar and Jupp*, 1999], wind erosion studies, and to locate wind turbines.

[18] **Acknowledgments.** We thank Michael Hobbins, David Jones, Nathan Gillett, Alan Beswick, Milton Woods and Chi-Fan Shih for helpful discussions; Jim Elliot, NOAA Earth System Research Laboratory and ECMWF for data access; and two reviewers for their helpful comments. The resultant daily surfaces are freely available from http://www-data.wron.csiro.au/ts/climate/wind/mcvicar_etal_grl2008.

References

Allan, R. P., and B. J. Soden (2007), Large discrepancy between observed and simulated precipitation trends in the ascending and descending branches of the tropical circulation, *Geophys. Res. Lett.*, *34*, L18705, doi:10.1029/2007GL031460.

Archer, C. L., and M. Z. Jacobson (2003), Spatial and temporal distributions of U. S. winds and wind power at 80 m derived from measurements, *J. Geophys. Res.*, *108*(D9), 4289, doi:10.1029/2002JD002076.

Aristidi, E., et al. (2005), An analysis of temperatures and wind speeds above Dome C, Antarctica, *Astron. Astrophys.*, *430*, 739–746.

Betts, A. K., M. Zhao, P. A. Dirmeyer, and A. C. M. Beljaars (2006), Comparison of ERA40 and NCEP/DOE near-surface data sets with other ISLSCP-II data sets, *J. Geophys. Res.*, *111*, D22S04, doi:10.1029/2006JD007174.

Bureau of Meteorology (2007), *Australian Daily Wind Data Product IDCJC*06.200706, Melbourne, Victoria, Australia.

Gillett, N. P., T. D. Kell, and P. D. Jones (2006), Regional climate impacts of the Southern Annular Mode, *Geophys. Res. Lett.*, *33*, L23704, doi:10.1029/2006GL027721.

Gupta, A. S., and M. H. England (2006), Coupled ocean-atmosphere-ice response to variations in the Southern Annular Mode, *J. Clim.*, *19*, 4457–4486.

Held, I. M., and B. J. Soden (2006), Robust responses of the hydrological cycle to global warming, *J. Clim.*, *19*, 5686–5699.

Hendon, H. H., D. W. J. Thompson, and M. C. Wheeler (2007), Australian rainfall and surface temperature variations associated with the Southern Hemisphere Annular Mode, *J. Clim.*, *20*, 2452–2467.

Hobbins, M. T. (2004), Regional evapotranspiration and pan evaporation: Complementary interactions and long-term trends across the conterminous United States, Ph.D. thesis, Colo. State Univ., Fort Collins.

Hutchinson, M. F. (2004), *ANUSPLIN Version 4.3 User Guide*, Cent. for Resour. and Environ. Stud., Aust. Natl. Univ., Canberra, A. C. T. (Available at http://cres.anu.edu.au/outputs/software.php)

Hutchinson, M. F., J. D. Kalma, and M. E. Johnson (1984), Monthly estimates of wind speed and wind run for Australia, *J. Climatol.*, *4*, 311–324.

Kalnay, E., et al. (1996), The NCEP/NCAR 40-year reanalysis project, *Bull. Am. Meteorol. Soc.*, *77*, 437–471.

Kanamitsu, M., W. Ebisuzaki, J. Woollen, S.-K. Yang, J. J. Hnilo, M. Fiorino, and G. L. Potter (2002), NCEP/DOE AMIP-II reanalysis (R-2), *Bull. Am. Meteorol. Soc.*, *83*, 1631–1643.

Klink, K. (1999), Trends in mean monthly maximum and minimum surface wind speeds in the coterminous United States, 1961 to 1990, *Clim. Res.*, *13*, 193–205.

Lorenz, D. J., and E. T. DeWeaver (2007), The response of the extratropical hydrological cycle to global warming, *J. Clim.*, *20*, 3470–3484.

Lu, J., G. A. Vecchi, and T. Reichler (2007), Expansion of the Hadley cell under global warming, *Geophys. Res. Lett.*, *34*, L06805, doi:10.1029/2006GL028443.

Lynch, A. H., J. A. Curry, R. D. Brunner, and J. A. Maslanik (2004), Toward an integrated assessment of the impacts of extreme wind events on Barrow, Alaska, *Bull. Am. Meteorol. Soc.*, *85*, 209–221.

McVicar, T. R., and D. L. B. Jupp (1999), Estimating one-time-of-day meteorological data from standard daily data as inputs to thermal remote sensing based energy balance models, *Agric. For. Meteorol.*, *96*, 219–238.

McVicar, T. R., T. G. Van Niel, L. Li, M. F. Hutchinson, X. Mu, and Z. Liu (2007), Spatially distributing monthly reference evapotranspiration and pan evaporation considering topographic influences, *J. Hydrol.*, *338*, 196–220.

Ozdogan, M., G. D. Salvucci, and B. T. Anderson (2006), Examination of the Bouchet-Morton complementary relationship using a mesoscale climate model and observations under a progressive irrigation scenario, *J. Hydrometeorol.*, *7*, 235–251.

Pérez, I. A., M. A. García, M. L. Sánchez, and B. de Torre (2005), Analysis and parameterisation of wind profiles in the low atmosphere, *Sol. Energy*, *78*, 809–821.

Pirazzoli, P. A., and A. Tomasin (2003), Recent near-surface wind changes in the central Mediterranean and Adriatic areas, *Int. J. Climatol.*, *23*, 963–973.

Pryor, S. C., R. J. Barthelmie, and E. S. Riley (2007), Historical evolution of wind climates in the USA, *J. Phys. Conf. Ser.*, *75*, 012065, doi:10.1088/1742-6596/75/1/012065. (Available at http://www.iop.org/EJ/toc/1742-6596/75/1)

Rayner, D. P. (2007), Wind run changes: The dominant factor affecting pan evaporation trends in Australia, *J. Clim.*, *20*, 3379–3394.

Rehman, S., and A. Ahmad (2004), Assessment of wind energy potential for coastal locations of the Kingdom of Saudi Arabia, *Energy*, *29*, 1105–1115.

Robeson, S. M., and K. A. Shein (1997), Spatial coherence and decay of wind speed and power in the north-central United States, *Phys. Geogr.*, *18*, 479–495.

Roderick, M. L., L. D. Rotstayn, G. D. Farquhar, and M. T. Hobbins (2007), On the attribution of changing pan evaporation, *Geophys. Res. Lett.*, *34*, L17403, doi:10.1029/2007GL031166.

Seidel, D. J., Q. Fu, W. J. Randel, and T. J. Reichler (2008), Widening of the tropical belt in a changing climate, *Nature Geosci.*, *1*, 21–24.

Shenbin, C., L. Yunfeng, and A. Thomas (2006), Climatic change on the Tibetan Plateau: Potential evapotranspiration trends from 1961–2000, *Clim. Change*, *76*, 291–319.

Smits, A., A. M. G. Klein Tank, and G. P. Können (2005), Trends in storminess over the Netherlands, 1962–2002, *Int. J. Climatol.*, *25*, 1331–1344.

Stull, R. B. (1988), *An Introduction to Boundary Layer Meteorology*, 666 pp., Kluwer Acad., Dordrecht, Netherlands.

Stull, R. B. (1994), A convective transport theory for surface fluxes, *J. Atmos. Sci.*, *51*, 3–22.

Tuller, S. E. (2004), Measured wind speed trends on the west coast of Canada, *Int. J. Climatol.*, *24*, 1359–1374.

Turner, J., S. R. Colwell, G. J. Marshall, T. A. Lachlan-Cope, A. M. Carleton, P. D. Jones, V. Lagun, P. A. Reid, and S. Iagovkina (2005), Antarctic climate change during the last 50 years, *Int. J. Climatol.*, *25*, 279–294.

Uppala, S. M., et al. (2005), The ERA-40 re-analysis, *Q. J. R. Meteorol. Soc.*, *131*, 2961–3012.

Wentz, F. J., L. Ricciardulli, K. Hilburn, and C. Mears (2007), How much more rain will global warming bring?, *Science*, *317*, 233–235.

Xu, C., L. Gong, T. Jiang, D. Chen, and V. P. Singh (2006a), Analysis of spatial distribution and temporal trend of reference evapotranspiration and pan evaporation in Changjiang (Yangtze River) catchment, *J. Hydrol.*, *327*, 81–93.

Xu, M., C.-P. Chang, C. Fu, Y. Qi, A. Robock, D. Robinson, and H. Zhang (2006b), Steady decline of East Asian Monsoon winds, 1969–2000: Evidence from direct ground measurements of wind speed, *J. Geophys. Res.*, *111*, D24111, doi:10.1029/2006JD007337.

Yin, J. H. (2005), A consistent poleward shift of the storm tracks in simulations of 21st century climate, *Geophys. Res. Lett.*, *32*, L18701, doi:10.1029/2005GL023684.

Zhang, Y. Q., C. M. Liu, Y. H. Tang, and Y. H. Yang (2007), Trends in pan evaporation and reference and actual evapotranspiration across the Tibetan Plateau, *J. Geophys. Res.*, *112*, D12110, doi:10.1029/2006JD008161.

R. J. Donohue, L. T. Li, and T. R. McVicar, CSIRO Land and Water and eWater Cooperative Research Centre, GPO Box 1666, Canberra, ACT 2601, Australia. (tim.mcvicar@csiro.au)

D. P. Rayner, Department of Earth Sciences, University of Gothenburg, Box 460, SE-405 30 Gothenburg, Sweden.

L. Ricciardulli, Remote Sensing Systems, 438 First Street, Santa Rosa, CA 95401, USA.

M. L. Roderick, Research School of Earth Sciences, Australian National University, Canberra, ACT 0200, Australia.

T. G. Van Niel, CSIRO Land and Water and eWater Cooperative Research Centre, Private Bag No. 5, Wembley, WA 6913, Australia.

Auxiliary material for Paper 2008GL035627

Wind speed climatology and trends for Australia, 1975-2006: Capturing the stilling phenomenon and comparison with near-surface reanalysis output

Tim R. McVicar[1*], Thomas G. Van Niel[2], LingTao Li[1], Michael L. Roderick[3], David P. Rayner[4], Lucrezia Ricciardulli[5] and Randall J. Donohue[1]

[1] CSIRO Land and Water and eWater Cooperative Research Centre, GPO Box 1666, Canberra, 2601, ACT, Australia

[2] CSIRO Land and Water and eWater Cooperative Research Centre, Private Bag No. 5, Wembley, 6913, WA, Australia

[3] Research School of Earth Sciences, Australian National University, Canberra, 0200, ACT, Australia

[4] Department of Earth Sciences, University of Gothenburg, Box 460, 405 30 Gothenburg, Sweden

[5] Remote Sensing Systems, 438 First Street, Santa Rosa, CA 95401, USA

McVicar, T.R., Van Niel, T.G., Li, L.T., Roderick, M.L., Rayner, D.P., Ricciardulli, L. and Donohue, R.J. (2008) Wind speed climatology and trends for Australia, 1975-2006: Capturing the stilling phenomenon and comparison with near-surface reanalysis output. *Geophysical Research Letters,* 35, L20403, doi:10.1029/2008GL035627.

October 2008

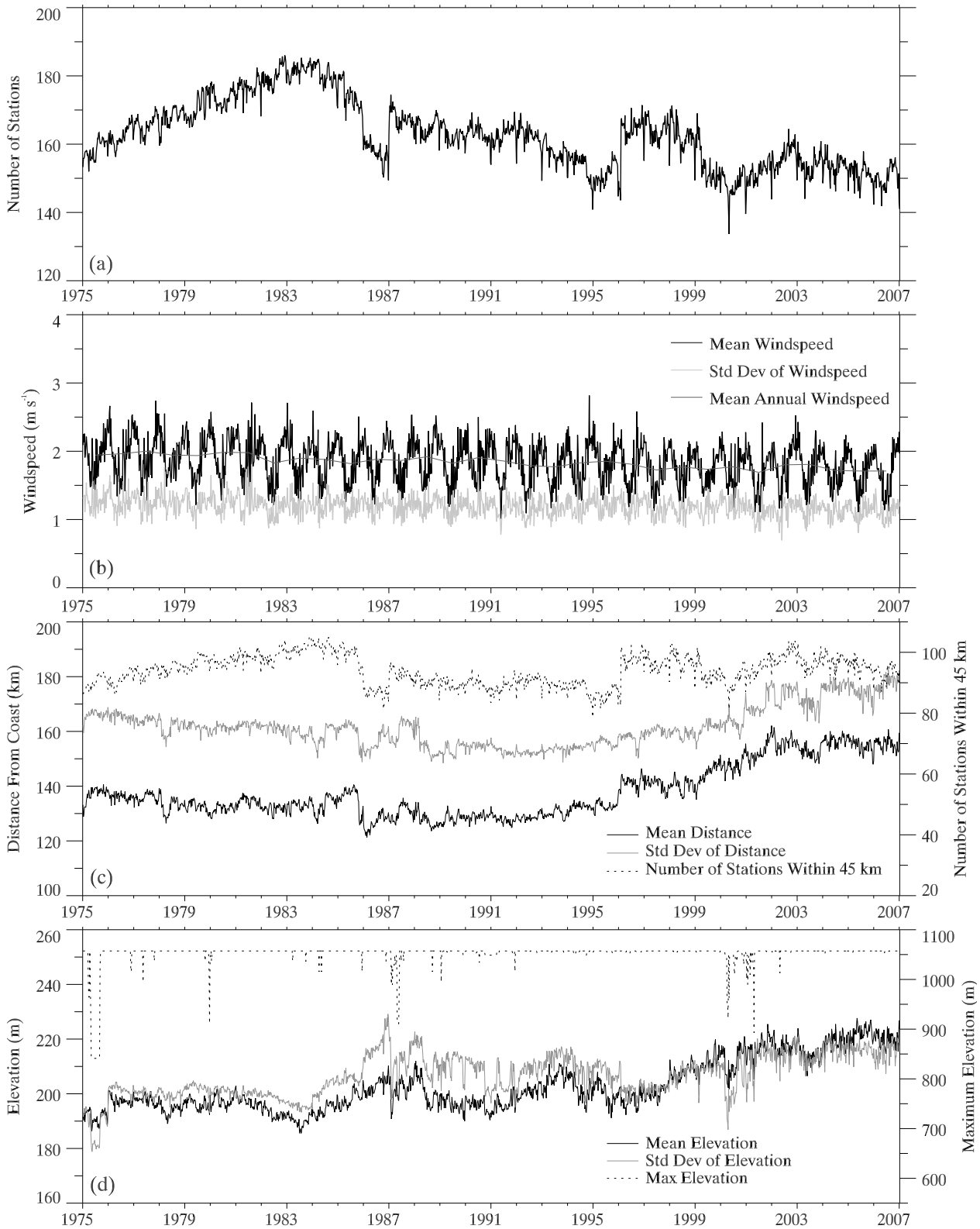

Auxiliary Figure S1. Basic characterisation of the *u* dataset: (a) shows the number of stations with 2 m high anemometers; (b) is the mean and standard deviation of *u*, and the mean annual *u*; (c) illustrates the mean and standard deviation of the distance from coast and the number of stations within 45 km from the coast; and (d) shows the mean, standard deviation and maximum station elevation. Weekly averages are shown for all variables, except the mean annual data shown in (b).

Auxiliary Table S1. For each of the plots using weekly averaged data in Auxiliary Figure S1 basic descriptive statistics are provided using daily data, except for the mean annual data shown in Auxiliary Figure S1b. The abbreviations Max., Min. and Std Dev. refer to the maximum, minimum and standard deviation, respectively.

Figure	Data	Max.	Min.	Mean	Std Dev.
Figure S1a	Number of stations	194	112	162.61	12.91
Figure S1b	Mean wind speed (m s^{-1})	4.24	0.83	1.84	0.42
Figure S1b	Mean Annual wind speed (m s^{-1})	2.00	1.69	1.84	0.09
Figure S1b	Std Dev. wind speed (m s^{-1})	2.69	0.53	1.19	0.24
Figure S1c	Mean distance from sea (km)	167.79	117.23	137.84	10.07
Figure S1c	Std Dev. sea distance (km)	188.53	133.18	161.67	7.80
Figure S1c	Number of stations within 45 km	111	65	93.95	7.17
Figure S1d	Mean elevation (m)	235.49	179.32	202.79	10.04
Figure S1d	Std Dev. of elevation (m)	234.31	174.66	206.63	8.38
Figure S1d	Max. elevation (m)	1057.26	709.70	1052.45	28.60

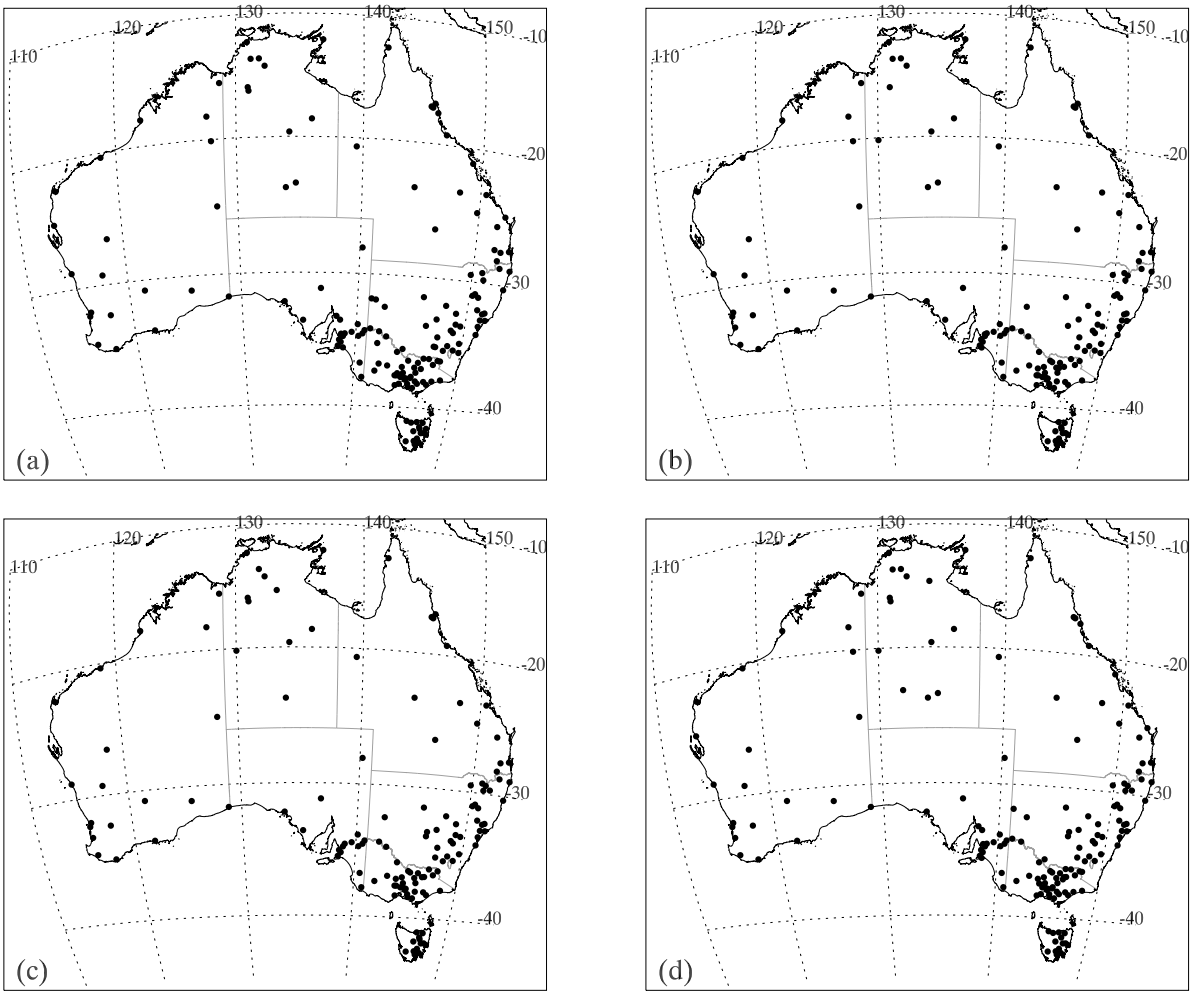

Auxiliary Figure S2. Location of input data for the 15th day of 2001 for: (a) January; (b) April; (c) July and (d) October, respectively.

Auxiliary Appendix S1: Spatially Interpolating Daily Wind Speed.

ANUSPLIN [Version 4.3 *Hutchinson*, 2004] is a software package developed to spatially interpolate hydrometeorological and climatological variables and to detect input data errors. It implements thin-plate spline interpolation [*Wahba and Wendelberger*, 1980] and the use of parametric sub-models [or covariates *Wahba*, 1990] called partial thin plate spline models. Wide-spread use of ANUSPLIN and its enhanced utility over other spatial interpolation approaches, including kriging, are summarised in *McVicar et al*. [2007]. In this study four models were evaluated to spatially interpolate *u*, namely:

1. bi-variate thin plate spline (BVTPS) as a function of longitude and latitude;
2. tri-variate thin plate spline (TVTPS) as a function of longitude, latitude and distance inland from coast [*Hutchinson et al.*, 1984];
3. tri-variate partial thin plate spline (TVPTPS) incorporating a BVTPS as a function of longitude and latitude and a constant linear dependence on elevation [*McVicar et al.*, 2007]; and
4. quart-variate partial thin plate spline incorporating a TVTPS as a function of longitude, latitude and distance inland from coast with and a constant linear dependence on elevation.

A transformation of distance from the coast (*d*) in km was applied to capture the impact of sea-breezes and land-breezes on *u*. Following *Hutchinson* [1984, pers comm. 1999] the transformation of distance inland from the coast (*d'*) was $d' = 30 \tanh(d/15)$ which essentially limits the impact of sea/land-breezes to within 45 km of the coast, denoted '*u* f (X, Y, *d'*)' in the following. On average 94 stations (Auxiliary Figure S1c) are within 45 km of the coast, for all stations the average elevation is 203 m with the highest station located at 1057 m (Auxiliary Figure S1d). Models 2 and 3 address perceived inadequacies of thin plate splines raised by Lou *et al.*, [2008] who did not allow for tri-variate spline (using the third variable as either another dependent variable [i.e., a TVTPS] or a covariate [i.e., a TVPTPS]) in their modelling (so they essentially used model 1 above). Additionally, it is anticipated that model 4 would better allow coastal-mountainous (i.e., mountainous areas that are within 45 km of the sea) areas to be modelled. This addresses a perceived limitation of splines raised by Lou *et al.*, [2008].

The four models were applied to the test year of 2001 (Auxiliary Figure S2 shows the spatial distribution of input data for the 15th day of four select months) with ANUSPLIN reporting several statistics that characterise its ability to fit the data, including the expected true mean

square error, T(m, λ), which is regarded as an optimistic measurement of error and the generalised cross-validation statistic, GCV(m, λ) considered a pessimistic, or conservative, measurement of error [*Hutchinson*, 2004]. When both errors are reported as a square root they have the units of the dependent variable. The order of the spline (m) and the smoothing parameter (λ) control the trade-off between the amount of data fidelity and surface roughness [*Hutchinson*, 2004], and λ is determined by minimising the GCV(m, λ) which has been previously used to find the 'best' model among competitors [*Davis*, 1987]. In all cases m = 2, and this 'best' model was successfully used to fit over 95% of the days. When this 'best' model failed to fit the data, or if any grid-cells had negative u values in resultant daily u surfaces, a square root transformation was applied to the dependent input data (i.e., daily u) prior to fitting the data with a spline, denoted '$u^{0.5}$ f (X, Y, d')' in the following. Hutchinson [1995] developed this strategy when fitting non-negative positively skewed precipitation data with ANUSPLIN successfully reducing model error. Here this strategy was used to fit another 494 days. For isolated days, for isolated stations if the residual between the input u data and the ANUSPLIN modelled value was greater than 3.6 times the error standard deviation, the average of the input u data and the modelled value was used as input to any subsequent iteration(s); this was performed a maximum of five times, allowing another 21 days to be fit. For the few remaining days that ANUSPLIN was unable to successfully fit a spline model, the 55 output surfaces were generated in ANUSPLIN, essentially by fitting the data with a multiple linear regression model (refer to Auxiliary Figure S3 and Auxiliary Table S2).

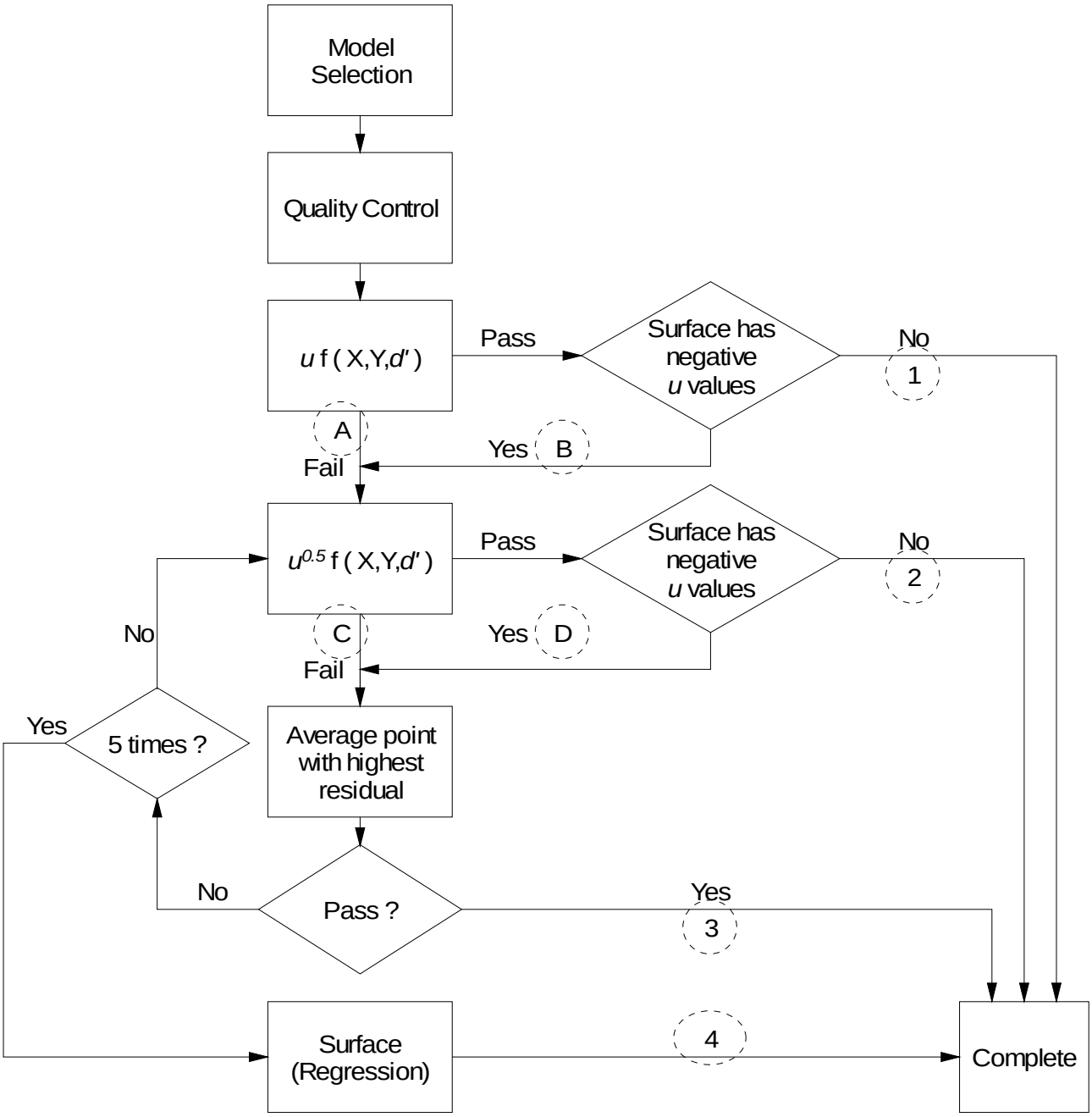

Auxiliary Figure S3. Flowchart of the methodology implemented to generate the 11,688 daily *u* surfaces. The numbered completed pathways identify the four ways a surface could be generated. Interim conditions are lettered. Yearly-based counts for each are provided in Auxiliary Table S2. The meaning of '*u* f (X, Y, *d*')' and '$u^{0.5}$ f (X, Y, *d*')' is explained in Auxiliary Appendix S1.

Auxiliary Table S2. For each year the number of days completed via each pathway, total days, and interim conditions are shown. The numbers 1 to 4 refer to pathways for completing a daily *u* surface and the letters A to D refer to the interim conditions; all pathways and conditions are identified on Auxiliary Figure S3.

Year	Completed Pathway				Total	Interim Condition			
	1	2	3	4	Days	A	B	C	D
1975	353	10	1	1	365	11	7	2	0
1976	343	20	1	2	366	28	1	3	0
1977	348	17	0	0	365	13	6	0	0
1978	354	9	0	2	365	10	4	2	0
1979	348	16	0	1	365	14	1	2	0
1980	342	20	0	4	366	17	9	4	0
1981	337	28	0	0	365	1	34	0	0
1982	349	16	0	0	365	5	10	0	0
1983	361	3	0	1	365	1	4	1	0
1984	351	12	0	3	366	7	7	4	0
1985	353	10	2	0	365	8	4	4	0
1986	363	1	1	0	365	5	1	2	0
1987	348	15	1	1	365	14	9	6	0
1988	356	7	1	2	366	7	10	3	0
1989	354	10	1	0	365	7	8	1	0
1990	354	10	0	1	365	3	9	0	0
1991	355	7	0	3	365	13	5	6	0
1992	342	23	0	1	366	14	13	1	0
1993	336	27	1	1	365	25	3	1	0
1994	335	28	0	2	365	28	4	3	0
1995	352	11	1	1	365	14	5	4	0
1996	338	25	2	1	366	10	22	3	0
1997	345	13	3	4	365	14	9	6	0
1998	349	10	1	5	365	15	2	8	0
1999	332	27	0	6	365	24	8	4	0
2000	320	40	2	4	366	43	14	14	0
2001	341	20	1	3	365	22	4	7	0
2002	350	12	0	3	365	11	2	3	0
2003	347	17	0	1	365	14	8	1	0
2004	353	12	0	1	366	7	5	2	0
2005	351	12	1	1	365	9	4	1	0
2006	357	6	1	1	365	9	0	4	0
Total	**11117**	**494**	**21**	**56**	**11688**	**371**	**200**	**77**	**0**

Auxiliary Table S3. For the test year (2001) the number of days with the lowest $\sqrt{GCV(m,\lambda)}$ and $\sqrt{T(m,\lambda)}$ statistic are tabulated.

Statistic	Spline Model *			
	1	2	3	4
$\sqrt{GCV(m,\lambda)}$	87	18	197	62
$\sqrt{T(m,\lambda)}$	238	72	30	25

* Full details of each spline model are provided in Auxiliary Appendix S1.

Auxiliary Table S4. Monthly average comparisons of $\sqrt{GCV(m,\lambda)}$ and $\sqrt{T(m,\lambda)}$ statistics for the 2001 test year for the spline models 1 and 2. The model with the lowest statistic for each month is bolded, and the observed *u* mean and standard deviation (Std Dev) are also provided. All units are m s^{-1}.

Month	Observed Statistics		Spline Model *			
			1		2	
	Mean	Std Dev	$\sqrt{GCV(m,\lambda)}$	$\sqrt{T(m,\lambda)}$	$\sqrt{GCV(m,\lambda)}$	$\sqrt{T(m,\lambda)}$
Jan	1.9374	0.2004	1.0132	**0.3555**	**0.9761**	0.3941
Feb	1.9636	0.2494	0.9901	**0.4005**	**0.9499**	0.4192
Mar	1.8007	0.1920	1.0070	**0.3395**	**0.9739**	0.4107
Apr	1.5613	0.2609	0.9327	**0.3148**	**0.9156**	0.3413
May	1.2191	0.2618	0.7384	**0.2589**	**0.7071**	0.3051
Jun	1.4475	0.3515	0.8596	**0.2955**	**0.8400**	0.3415
Jul	1.2792	0.2732	0.8382	**0.2876**	**0.8263**	0.3250
Aug	1.7702	0.4840	1.0106	**0.3307**	**0.9976**	0.3811
Sep	1.6758	0.3622	0.9287	**0.3286**	**0.9033**	0.3545
Oct	1.8354	0.2596	0.9620	**0.3346**	**0.9389**	0.3554
Nov	1.8911	0.2896	0.9785	**0.3410**	**0.9250**	0.3993
Dec	1.9251	0.3011	0.9554	**0.3414**	**0.9290**	0.3931

* Full details of each spline model are provided in Auxiliary Appendix S1.

Auxiliary Table S5. Frequency distributions (minimum, maximum and key percentiles) of the annual, seasonal and monthly *u* climatologies generated for 1975-2006 over all Australia; all units are m s^{-1}.

Time	Min	1%	5%	10%	25%	50%	75%	90%	95%	99%	Max
Annual	1.1	1.2	1.4	1.5	1.7	1.9	2.3	2.6	2.7	2.9	3.5
DJF	1.1	1.2	1.4	1.6	1.9	2.3	2.7	3.1	3.2	3.6	4.5
MAM	1.0	1.1	1.2	1.3	1.6	1.8	2.1	2.3	2.4	2.6	3.1
JJA	1.0	1.2	1.3	1.4	1.5	1.7	1.9	2.1	2.2	2.4	2.9
SON	1.3	1.4	1.5	1.6	1.9	2.1	2.4	2.8	2.9	3.1	3.9
Jan	1.1	1.2	1.4	1.6	1.9	2.3	2.7	3.1	3.3	3.6	4.7
Feb	1.0	1.1	1.3	1.5	1.8	2.2	2.6	3.1	3.2	3.6	4.3
Mar	0.9	1.0	1.2	1.4	1.7	2.0	2.3	2.7	2.8	3.1	3.8
Apr	0.9	1.1	1.2	1.3	1.5	1.8	2.0	2.2	2.3	2.5	3.0
May	0.9	1.0	1.2	1.3	1.4	1.6	1.8	2.0	2.1	2.3	2.8
Jun	0.9	1.1	1.2	1.3	1.5	1.6	1.8	2.0	2.1	2.3	2.9
Jul	1.0	1.2	1.3	1.3	1.5	1.6	1.8	2.1	2.2	2.4	2.9
Aug	1.1	1.3	1.4	1.4	1.6	1.8	2.0	2.3	2.4	2.5	2.9
Sep	1.2	1.4	1.5	1.6	1.7	2.0	2.2	2.5	2.6	2.8	3.3
Oct	1.2	1.4	1.5	1.7	1.9	2.1	2.5	2.8	2.9	3.1	4.1
Nov	1.2	1.3	1.5	1.7	1.9	2.3	2.6	3.0	3.1	3.4	4.4
Dec	1.2	1.3	1.5	1.6	1.9	2.3	2.6	3.0	3.2	3.5	4.7

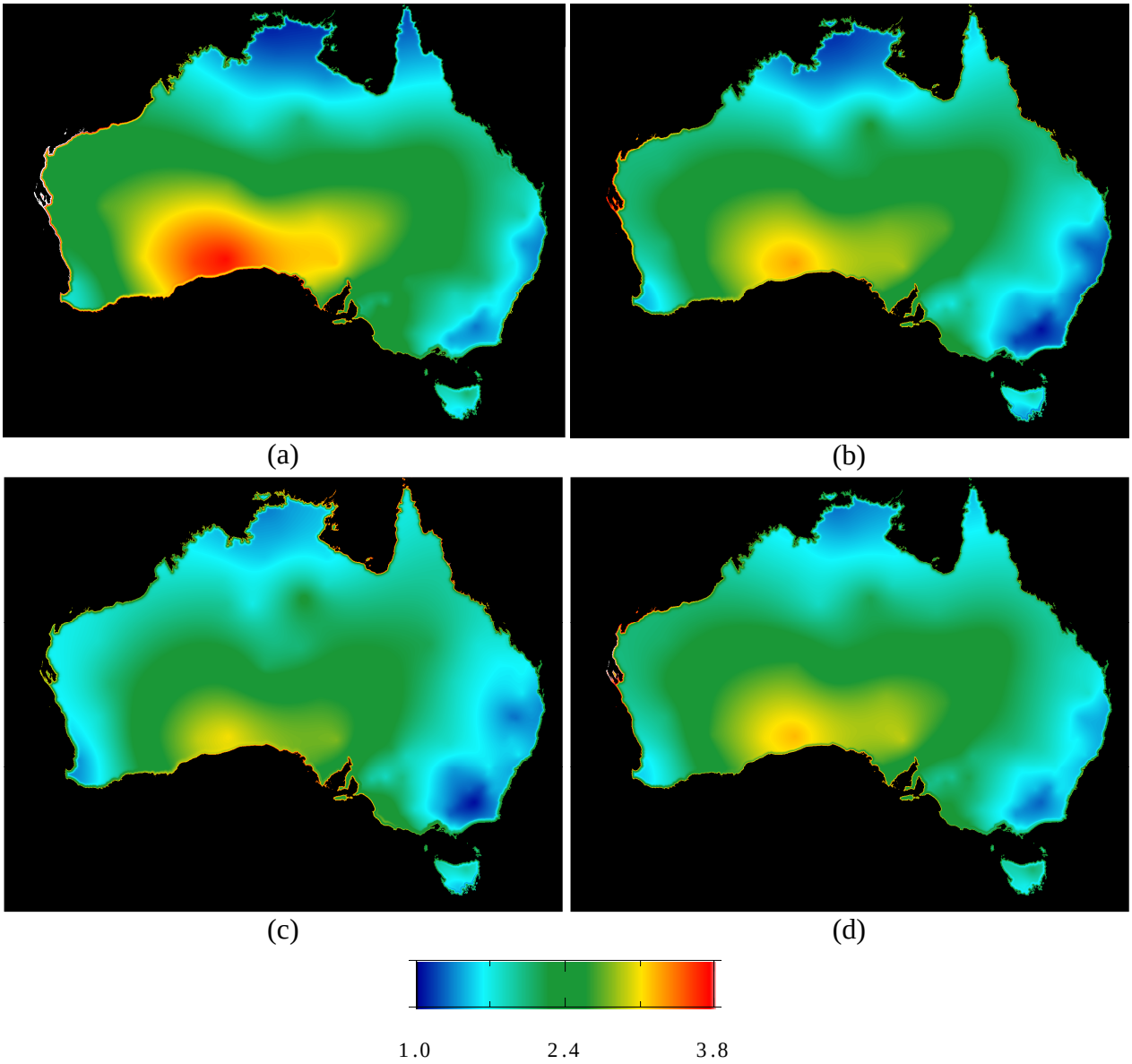

Auxiliary Figure S4. Seasonal climatologies of *u* for: (a) summer (DJF); (b) autumn (MAM); (c) winter (JJA) and spring (SON) for the period 1975 to 2006; all units are m s^{-1}.

Auxiliary Table S6. Frequency distributions (minimum, maximum and key percentiles) of the annual, seasonal and monthly *u* trends generated for 1975-2006 over all Australia; these units are m s^{-1} a^{-1}. The percentage of grid-cells with: (i) a negative trend; (ii) a significant (P = 0.05) trend; and (iii) a negative and significant (P = 0.05) trend are also shown. Results here are for the trends only; they are independent of the wind speed histograms presented in Auxiliary Table S5.

Time	Min	1%	5%	10%	25%	50%	75%	90%	95%	99%	Max	Area neg. Trend (%) *	Area sig. Trend (%) **	Area neg. and sig. Trend (%) ***
Annual	-0.058	-0.027	-0.019	-0.017	-0.013	-0.009	-0.006	0.001	0.005	0.012	0.031	88.56	59.62	57.56
DJF	-0.064	-0.039	-0.025	-0.022	-0.017	-0.013	-0.009	-0.001	0.004	0.013	0.040	91.48	77.58	75.78
MAM	-0.059	-0.028	-0.021	-0.018	-0.012	-0.007	-0.003	0.003	0.007	0.014	0.028	84.24	48.42	44.56
JJA	-0.050	-0.021	-0.016	-0.014	-0.010	-0.006	-0.002	0.003	0.006	0.012	0.027	81.29	39.33	36.00
SON	-0.058	-0.025	-0.018	-0.017	-0.015	-0.010	-0.006	0.001	0.005	0.012	0.035	88.77	66.84	64.92
Jan	-0.068	-0.039	-0.026	-0.023	-0.019	-0.016	-0.010	-0.002	0.004	0.012	0.041	91.75	78.15	76.70
Feb	-0.069	-0.051	-0.034	-0.029	-0.019	-0.011	-0.007	-0.001	0.005	0.014	0.042	90.89	74.64	72.29
Mar	-0.064	-0.032	-0.022	-0.019	-0.012	-0.007	-0.003	0.003	0.008	0.017	0.035	84.77	62.97	60.06
Apr	-0.052	-0.027	-0.023	-0.020	-0.014	-0.006	-0.002	0.005	0.009	0.016	0.026	80.62	74.54	67.74
May	-0.060	-0.027	-0.019	-0.016	-0.012	-0.007	-0.003	0.002	0.006	0.012	0.027	85.43	71.59	66.65
Jun	-0.044	-0.018	-0.014	-0.012	-0.008	-0.003	0.001	0.006	0.009	0.016	0.032	70.72	43.27	38.61
Jul	-0.052	-0.024	-0.016	-0.014	-0.011	-0.006	-0.003	0.002	0.005	0.010	0.021	84.72	52.71	47.47
Aug	-0.055	-0.022	-0.018	-0.016	-0.011	-0.007	-0.003	0.003	0.007	0.012	0.029	85.49	50.48	47.37
Sep	-0.059	-0.022	-0.018	-0.016	-0.013	-0.009	-0.005	0.001	0.004	0.010	0.033	88.78	24.58	19.80
Oct	-0.059	-0.025	-0.020	-0.019	-0.016	-0.011	-0.007	0.001	0.006	0.013	0.036	88.65	49.42	46.93
Nov	-0.057	-0.032	-0.021	-0.018	-0.016	-0.010	-0.006	0.002	0.006	0.014	0.035	87.58	47.80	43.97
Dec	-0.059	-0.028	-0.020	-0.017	-0.014	-0.011	-0.008	-0.001	0.005	0.013	0.038	91.14	60.98	59.34

* % surface where trend < 0 m s^{-1} a^{-1}

** % surface where trend is significant at the 95% level (P = 0.05) using a two-tailed t-test

*** % surface where trend < 0 m s^{-1} a^{-1} and where trend is significant at the 95% level (P = 0.05) using a two-tailed t-test

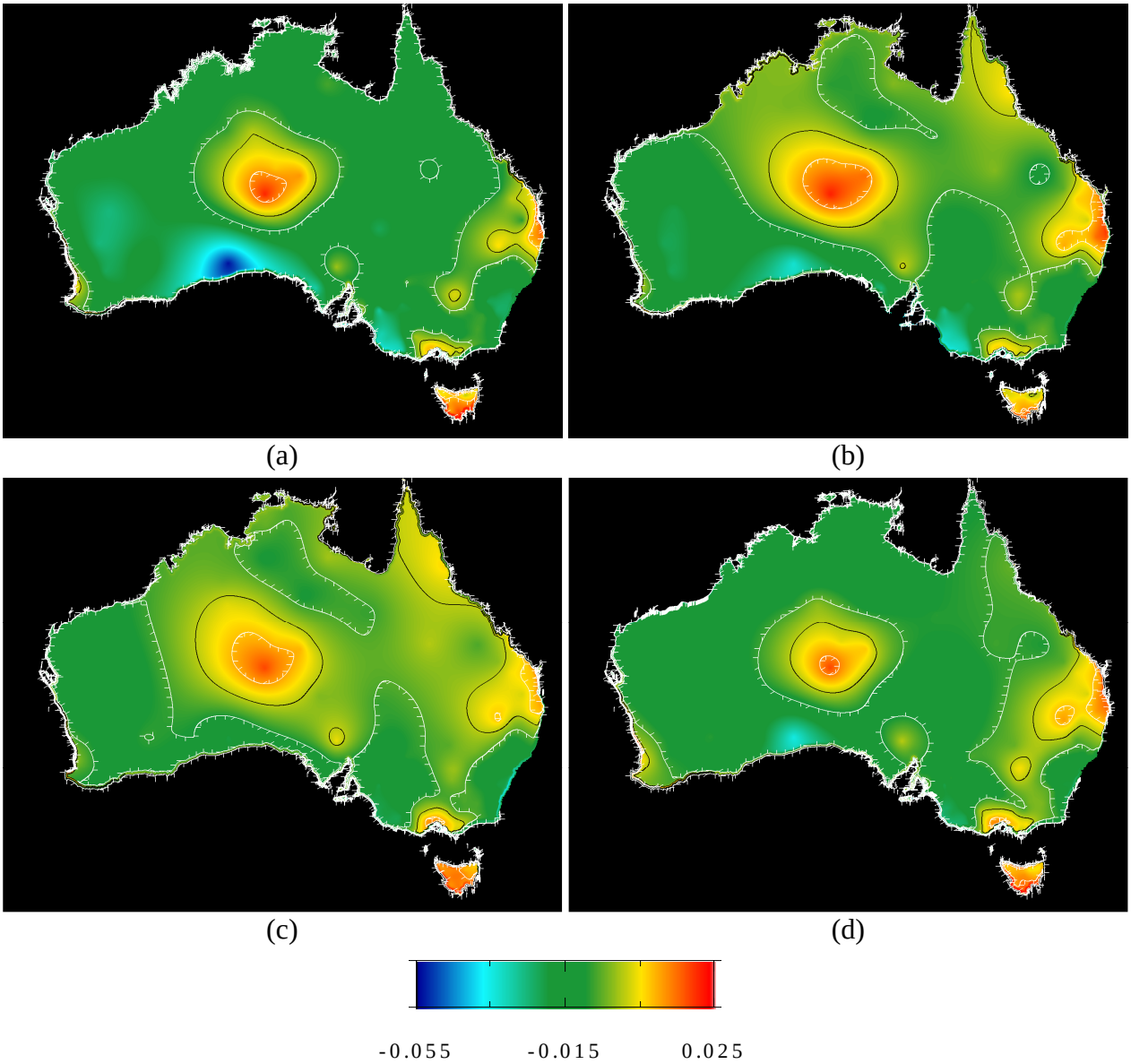

Auxiliary Figure S5. Seasonal trends of *u* for: (a) summer (DJF); (b) autumn (MAM); (c) winter (JJA) and spring (SON) for 1975-2006; all units are m s^{-1} a^{-1}. The black lines show where the trend is 0.0 m s^{-1} a^{-1} (i.e., where it changes between positive and negative), and the white lines show were the trends change from being non-significant to significant at the P = 0.05 level, with the white barbs pointing in the direction of significance.

Auxiliary Table S7. Basic statistics of the land-only grid-cells 1979-2001 annual *u* climatology and trends; the units of the climatology data are m s^{-1} and the units of the trend data are m s^{-1} a^{-1}. To minimise differences between the datasets, our 0.01° resolution data were resampled to the 2° resolution, and only the 'land-only grid-cells' (i.e., where all 40,000 grid-cells at 0.01° resolution are land in each 2° resolution grid-cell) were used to calculate the statistics.

Source	Mean	Std Dev	Max.	Min.	Num grid-cells	Mean relative our mean
Climatology						
Our study	2.01	0.37	2.97	1.31	146	1.00
NCEP/DOE	4.28	0.66	5.42	2.52	146	2.13
NCEP/NCAR	3.42	0.63	4.41	1.93	146	1.70
ERA40	3.68	0.48	4.98	2.38	146	1.83
Trends						
Our study	-0.013	0.009	0.018	-0.044	146	1.00
NCEP/DOE	-0.002	0.007	0.011	-0.038	146	0.15
NCEP/NCAR	-0.004	0.004	0.005	-0.019	146	0.31
ERA40	-0.002	0.007	0.034	-0.020	146	0.15

References

Davis, B. M. (1987), Uses and Abuses of Cross-Validation in Geostatistics, *Math. Geol.*, *19*, 241-248.

Hutchinson, M. F. (1995), Interpolating mean rainfall using thin plate smoothing splines, *Int. J. Geogr. Info. Sci.*, *9*, 385-403.

Hutchinson, M. F. (2004), ANUSPLIN Version 4.3 User Guide, http://cres.anu.edu.au/outputs/software.php, edited, The Australian National University, Centre for Resource and Environmental Studies, Canberra.

Hutchinson, M. F., J. D. Kalma, and M. E. Johnson (1984), Monthly Estimates of Wind Speed and Wind Run for Australia, *J. Climatol.*, *4*, 311-324.

Luo, W., M. C. Taylor, and S. R. Parker (2008), A comparison of spatial interpolation methods to estimate continuous wind speed surfaces using irregularly distributed data from England and Wales, *Int. J. Climatol.*, *28*, 947-959.

McVicar, T. R., T. G. Van Niel, L. Li, M. F. Hutchinson, X. Mu, and Z. Liu (2007), Spatially distributing monthly reference evapotranspiration and pan evaporation considering topographic influences, *J. Hydrol.*, *338*, 196-220.

Wahba, G. (1990), *Spline Models for Observational Data*, 169 pp., Society for Industrial and Applied Mathematics, Philadelphia, Pennsylvania.

Wahba, G., and J. Wendelberger (1980), Some New Mathematical Methods for Variational Objective Analysis Using Splines and Cross Validation, *Mon. Weath. Rev.*, *108*, 1122-1143.